KLOE NOTE n^{o}224
April 2011

Measurement of the branching ratio of $\eta \to e^+e^-e^+e^-(\gamma)$ decay

S. Giovannella [a] and R. Versaci [b]

[a] *Laboratori Nazionali di Frascati dell'INFN, Frascati, Italy.*

[b] *CERN, Geneva, Switzerland*

Abstract

We have measured the branching fraction of the decay $\eta \to e^+e^-e^+e^-(\gamma)$ using 1733 pb^{-1} of 2004-2005 data. This large dataset allowed us to have 362 ± 29 signal events at the end of the analysis. These correspond to $\mathrm{B}R(\eta \to e^+e^-e^+e^-(\gamma)) = (2.44 \pm 0.19_{\mathrm{stat.}} \pm 0.04_{\mathrm{norm.}} {}^{+0.10}_{-0.08\ \mathrm{syst.}}) \cdot 10^{-5}$. Two upper limits for the branching ratio from CMD-2 and WASA are reported in literature.

Contents

1 Introduction

As for the already studied decay $\eta \to \pi^+\pi^- e^+ e^-$ [1,2], the use of the virtual photon allows to probe the structure of the η meson and the interaction in the time-like region of four momentum transfer square, q^2, which is equal to the squared invariant mass of the lepton pair. Also, the lack of hadrons among the decay products, makes the matrix element directly sensitive to the η meson form factor which is interesting because the pseudoscalar exchange is the major contribution to the hadronic light-by-light scattering part of the muon anomalous magnetic moment. More generally this decay allows to investigate the Chiral Perturbation Theory (χPT) [3–7].
The presently available theoretical predictions [4–8] and experimental results [9–11] are reported in table 1 and 2 respectively.

	$\frac{\Gamma(\eta\to e^+e^-e^+e^-)}{\Gamma(\eta\to\gamma\gamma)}$	$BR(\eta \to e^+e^-e^+e^-)$
Jarlskog-Pilkuhn (1967)	$6.6 \cdot 10^{-5}$	$2.59 \cdot 10^{-5}$
Miyazaki-Takasugi (1973)	$6.14 \cdot 10^{-5}$	$2.41 \cdot 10^{-5}$
Bijnens-Persson (1999)	$(6.40 \pm 0.02) \cdot 10^{-5}$	$2.52 \cdot 10^{-5}$
Bijnens-Persson (1999)	$(6.73 \pm 0.02) \cdot 10^{-5}$	$2.65 \cdot 10^{-5}$
Bijnens-Persson (1999)	$(6.71 \pm 0.02) \cdot 10^{-5}$	$2.64 \cdot 10^{-5}$
Bijnens-Persson (1999)	$(6.64 \pm 0.02) \cdot 10^{-5}$	$2.61 \cdot 10^{-5}$
Lih (2009)	-	$2.47 \cdot 10^{-5}$
Bijnens-Petri (2010)	$6.453 \cdot 10^{-5}$	$2.54 \cdot 10^{-5}$
Bijnens-Petri (2010)	$(6.800 \pm 0.013) \cdot 10^{-5}$	$2.67 \cdot 10^{-5}$
Bijnens-Petri (2010)	$(6.770 \pm 0.016) \cdot 10^{-5}$	$2.66 \cdot 10^{-5}$

Table 1
Summary of the theoretical predictions present in literature. All but one (Lih 2009 [6]) provide the ratio $\Gamma(\eta \to e^+e^-e^+e^-)/\Gamma(\eta \to \gamma\gamma)$; for these cases we have obtained the branching ratio dividing for the $BR(\eta \to \gamma\gamma)$ presently reported by the PDG [11] ($BR(\eta \to \gamma\gamma) = 0.3931 \pm 0.0020$). The various Bijnens-Persson and Bijnens-Petri entries correspond to different η form factors and Vector Meson Dominance (VMD) assumptions respectively.

	$BR(\eta \to e^+e^-e^+e^-)$
Akhmetshin *et al.* (2008) [CMD-2]	$< 6.9 \cdot 10^{-5}$ at 90% C.L.
Berlowski *et al.* (2008) [WASA]	$< 9.7 \cdot 10^{-5}$ at 90% C.L.

Table 2
Summary of the available experimental results.

2 Data sample

For this analysis the ETA4CTAG selection algorithm [12] has been required. Therefore only data and MC processed with datarec version 26 or higher [13] are used in the analysis, corresponding to the following samples:

- 167531 pb^{-1} of signal Monte Carlo, private production, including run by run background simulation [14]. It has been used for the signal shape and the efficiency. The matrix element used for the signal Monte Carlo is the one quoted in reference [5]. The package PHOTOS [15] has been used to account for Final State Radiation photons.

- 3447 pb^{-1} of Monte Carlo `all_phys` 2004-2005, used for background shape and studies:
  · 1715 pb^{-1} of `all_phys` MC (`dtr_gb_nr=0`), having LSF = 1 ;
  · 1718 pb^{-1} of `all_phys2` MC (`dtr_gb_nr=1`), having LSF = 0.5 ;
  · 1745 pb^{-1} of `all_phys3` MC (`dtr_gb_nr=2`), having LSF = 0.5 .
  We have used this sample to study the background coming from the three main decays of the ϕ meson: $\phi \to K^+K^-$, $\phi \to K^0_S K^0_L$ and $\phi \to \pi^+\pi^-\pi^0$. The background from the remaining ϕ decays has been studied using the `allrad` Monte Carlo sample.

- 17517 pb^{-1} of Monte Carlo `allrad` 2004-2005 (LSF = 10) used for background shape and studies. We have used this sample to study the background coming from the remaining ϕ decays, i.e. $\phi \to \eta\gamma$ and other minor decay modes.

- 1733 pb^{-1} of data from 2004-2005 dataset.

- 243 pb^{-1} of off-peak ($\sqrt{s} = 1000\ MeV$) data from 2006 dataset. This sample is used to study the background from continuum events.

During the event selection the recover splitting procedure has been applied. The cluster energy correction described in reference [16] has been applied to all the Monte Carlo samples.

3 Event selection

3.1 Event classification

The ETA4CTAG selection algorithm has been used for this analysis. The algorithm is described in the KLOE memo 329 [12] and summarized here. The requirements are:

(1) at least four tracks with Point of Closest Approach (PCA) inside the Fiducial Volume (FV), defined as a cylinder centered in the origin and having radius $R = 4$ cm and height $h = 20$ cm;
(2) at least one prompt neutral cluster, having energy $E_{cl} \geq 250$ MeV;
(3) zero prompt neutral clusters, having energy in the range $50 \leq E_{cl} \leq 250$ MeV.

The clusters have to be in the polar angle range $(23°, 157°)$. A cluster is defined neutral if:

- it does not have any associated track;
- it is in time, *i.e.* satisfies the requirement:

$$|t - r/c| < min(5\ \sigma_t,\ 2\ ns) \tag{1}$$

$$\text{where} \qquad \sigma_t = \frac{54\ ps}{\sqrt{E[GeV]}} \oplus 100\ ps. \tag{2}$$

3.2 Track selection

The first step of the analysis is to identify four track candidates. Only tracks coming from the FV around the Interaction Point (IP) are taken into account. It could happen that, because of reconstruction problem, the track of a particle is split. In order to avoid to select as candidates two tracks corresponding to the same particle, a check on so-called "broken tracks" is performed. All the possible pairs of tracks, in all the four combination of First and Last Hit (FH-FH, FH-LH LH-FH, LH-LH) are considered. If any combination satisfies both the checks on the differences of the momenta:

$$\Delta p_T < 4.5\ MeV \tag{3}$$

$$\Delta p_z < 3.0\ MeV \tag{4}$$

the two tracks are considered as coming from the same particle. The track having the farthest PCA to the IP is flagged as broken and vetoed as candidate.

At least two positive and two negative track candidates are required. The two tracks, per charge, with the highest momenta are selected for the analysis.

4 Efficiencies

The selection efficiency has been evaluated on the signal MC once a data-MC correction for the tracking has been applied.
The measurement of this correction has been performed using $\phi \to \pi^+\pi^-\pi^0$ events from the UFO stream and the corresponding MC samples. The corrections have been evaluated as functions of P_t and P_z and have been found to be about 1%. Then, these have been applied to each track (before track selection) as function of P_t and P_z.
A more detailed description of the tracking efficiency studies can be found in the KLOE memo 343 [17].
It could be argued that applying to the electrons a correction evaluated using a pion control sample could introduce some bias. The relative difference between the corrections for pions and electrons is at most 5% [18], which corresponds to a difference of $O(10^{-4})$ in the efficiency. Since our final statistical uncertainty is more than two orders of magnitude larger, our assumption is justified.
The trigger efficiency has been evaluated by Monte Carlo after both the event selection and the tracking efficiency corrections are applied: $\epsilon_{\rm trg} = 0.998(4)$.

5 Background rejection

The study for background rejection has profited of the knowledge gained with the $\eta \to \pi^+\pi^-e^+e^-$ analysis [1,2]. A similar approach has been used for the channel under study.
We have started studying the KLOE official MC productions `all_phys` (for $\phi \to K^+K^-$, $\phi \to K^0_S K^0_L$, and $\phi \to \pi^+\pi^-\pi^0$ decays) and `allrad` (for $\phi \to \eta\gamma$ and minor ϕ decays). We have used as well the data collected at $\sqrt{s} = 1\ GeV$ to study background contamination from continuum.
After the Event Classification (EVCL), the main background comes from the $\phi \to \pi^+\pi^-\pi^0$ decay with a π^0 undergoing a Dalitz decay, therefore having four tracks coming from the interaction point. The same happens for the $\phi \to \eta\gamma$ with $\eta \to \pi^+\pi^-\pi^0$ decay chain. Other backgrounds due to η decays, worth to be studied because they can mimic the signal, are $\eta \to \pi^+\pi^-e^+e^-$, $\eta \to \pi^+\pi^-\gamma$, $\eta \to e^+e^-\gamma$ and $\eta \to \gamma\gamma$ with the photons converting in the Beam Pipe (BP) and/or in the Drift Chamber Wall (DCW). Another important source of background is given by Bhabha scattering events not properly reconstructed.

The composition of the background after the event classification is shown in table 3.

Decay chain	Event selected	Sample	LSF
$\eta \to e^+e^-e^+e^-$	8199	`allrad`	10
$\phi \to K^+K^-$	62665	`all_phys`	1
$\phi \to K^0_S K^0_L$	50242	`all_phys`	1
$\phi \to \pi^+\pi^-\pi^0$	397672	`all_phys`	1
$\eta \to \pi^+\pi^-e^+e^-$	34370	`allrad`	10
$\eta \to \pi^+\pi^-\gamma$	16960	`allrad`	10
$\eta \to e^+e^-\gamma$	6844	`allrad`	10
$\eta \to \gamma\gamma$	1947	`allrad`	10
Other η decays	92636	`allrad`	10
Continuum	23180	Offpeak data	-

Table 3
Number of events selected after EVCL for the most important decay chains for this analysis. The sample used for the calculation (and the corresponding luminosity scale factor for MC) are also reported.

5.1 Cut on the momenta

The first cut of the analysis is on the sum of the absolute value of the momenta of the four selected tracks, $s4p = \sum_1^4 |\vec{p}_i|$. The following condition has to be satisfied:

$$600 < s4p < 700\ MeV\ . \tag{5}$$

The spectra of $s4p$ are shown in figure 1 for the five samples considered. The signal has an evident narrow peak compared to the backgrounds.

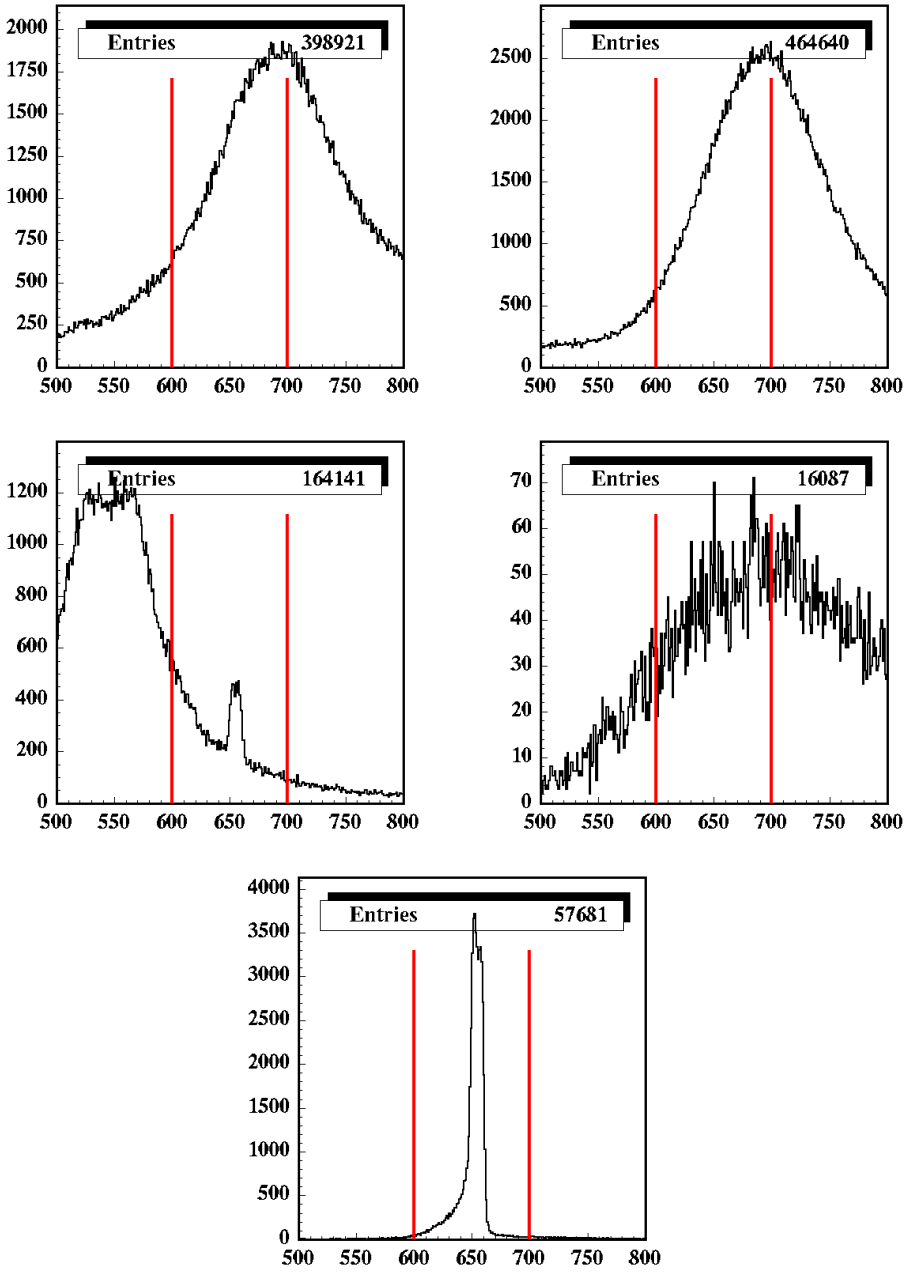

Fig. 1. Distribution of the sum of the absolute value of the momenta of the four selected tracks, *s4p*. Top left: data; top right: `all_phys` Monte Carlo; center left: `allrad` Monte Carlo; center right: offpeak data; bottom: signal Monte Carlo. The red lines show the cut applied.

5.2 Cut on "low θ" events

We apply a cut on "low θ" events. These events have one track in one direction and the other three and the photon in the opposite one. Also, the three tracks on the same side have a common origin around the QCAL modules. It

is reasonable to suppose that this kind of events are Bhabha events where an electron/positron interacts in some material around QCAL. This hypothesis is supported by the fact that the time of flight of all particles connected to a calorimeter cluster identifies them as electron.
The two quantities $\langle\cos\theta_f\rangle$ and $\langle\cos\theta_b\rangle$ have been defined as the average polar angle of forward and backward tracks and photon identified as signal. Distributions of $\langle\cos\theta_b\rangle$ vs $\langle\cos\theta_f\rangle$ are shown in figure 2. Events satisfying the logical AND of the two following conditions have been discarded:

$$\langle\cos\theta_f\rangle > 0.85 \tag{6}$$
$$\langle\cos\theta_b\rangle < -0.85 \tag{7}$$

5.3 Kinematic fit

We perform a kinematic fit on the remaining events in order to improve the event reconstruction resolution. The four-momentum conservation and the timing of the cluster are imposed as constraints:

$$P(e^+_{beam}) + P(e^-_{beam}) = P(e^+) + P(e^-) + P(e^+) + P(e^-) + P(\gamma) \tag{8}$$
$$T_\gamma = R_\gamma/c\ . \tag{9}$$

A loose cut on the χ^2 of the kinematic fit is applied in order to discard poorly reconstructed events having $\chi^2_{KF} > 4000$. The χ^2 distribution is shown in figure 3.

5.4 $\eta \to e^+e^-\gamma$ background

The $\eta \to e^+e^-\gamma$ decay is a source of background because the photon can convert either on the BP or the DCW, generating an e^+e^- pair. Then, if it is possible to extrapolate the corresponding tracks backward to the IP (see figure 4), this decay simulates the signal: $\eta \to e^+\ e^-\ \gamma \to e^+e^-e^+e^-$.
At the creation point, the distance between the two tracks is minimum and the invariant mass is almost zero. This fact can be exploited to develop a good background rejection algorithm. We extrapolate the electron and positron tracks backward from the Drift Chamber (DC) to the IP and calculate their invariant mass (M_{ee}) and their distance (D_{ee}) at the IP and at the intersections with the BP and DC. This is done for all of the four e^+e^- pairs of the event.

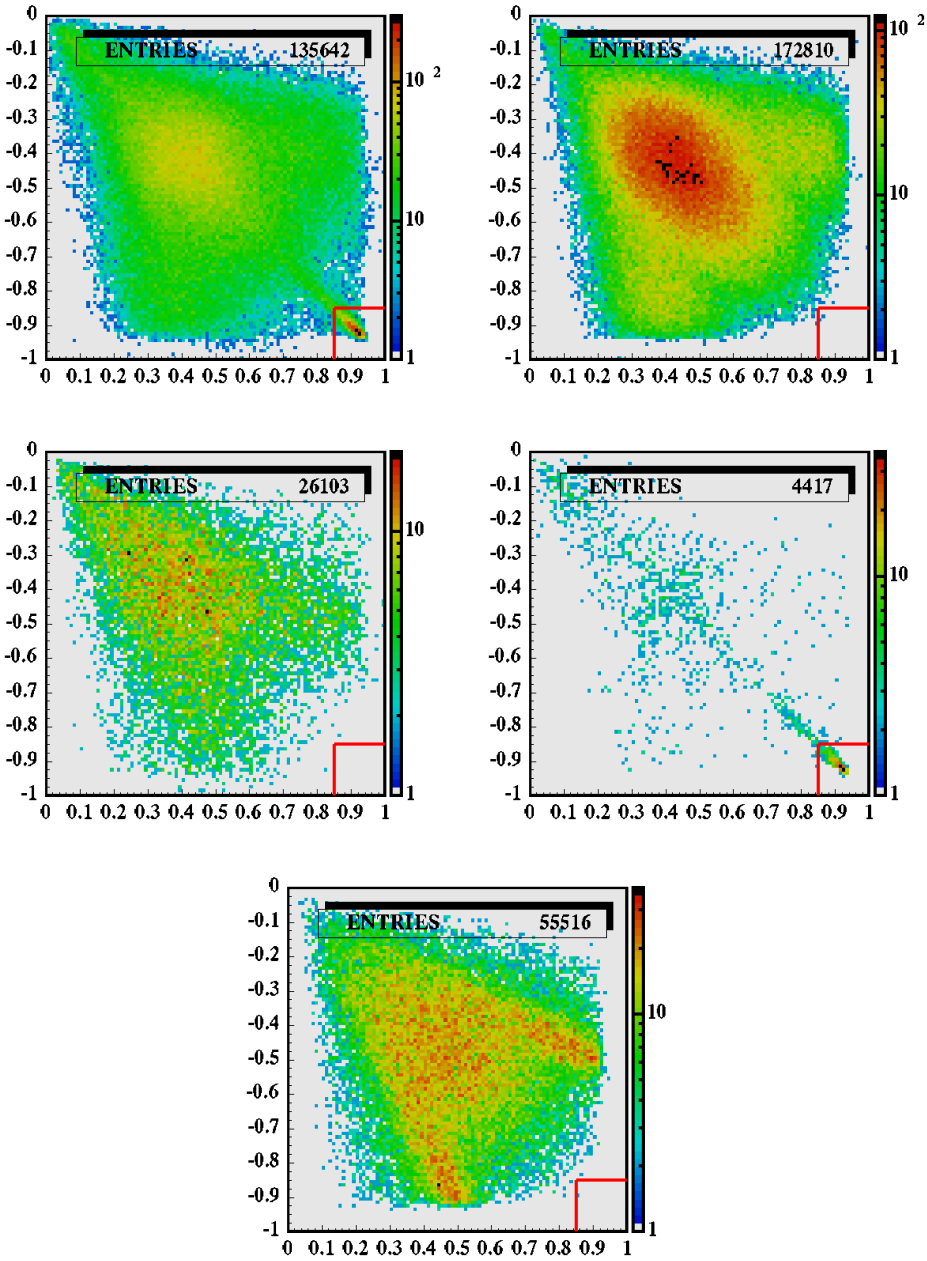

Fig. 2. $\langle \cos\theta_b \rangle$ vs $\langle \cos\theta_f \rangle$ distribution after $s4p$ cut. Top left: data; top right: `all_phys` Monte Carlo; center left: `allrad` Monte Carlo; center right: offpeak data; bottom: signal Monte Carlo. The red lines show the cut applied.

We reject events having at least one pair satisfying:

$$M_{ee}(BP) < 10\ MeV \text{ and} \tag{10}$$
$$D_{ee}(BP) < 2\ cm\ . \tag{11}$$

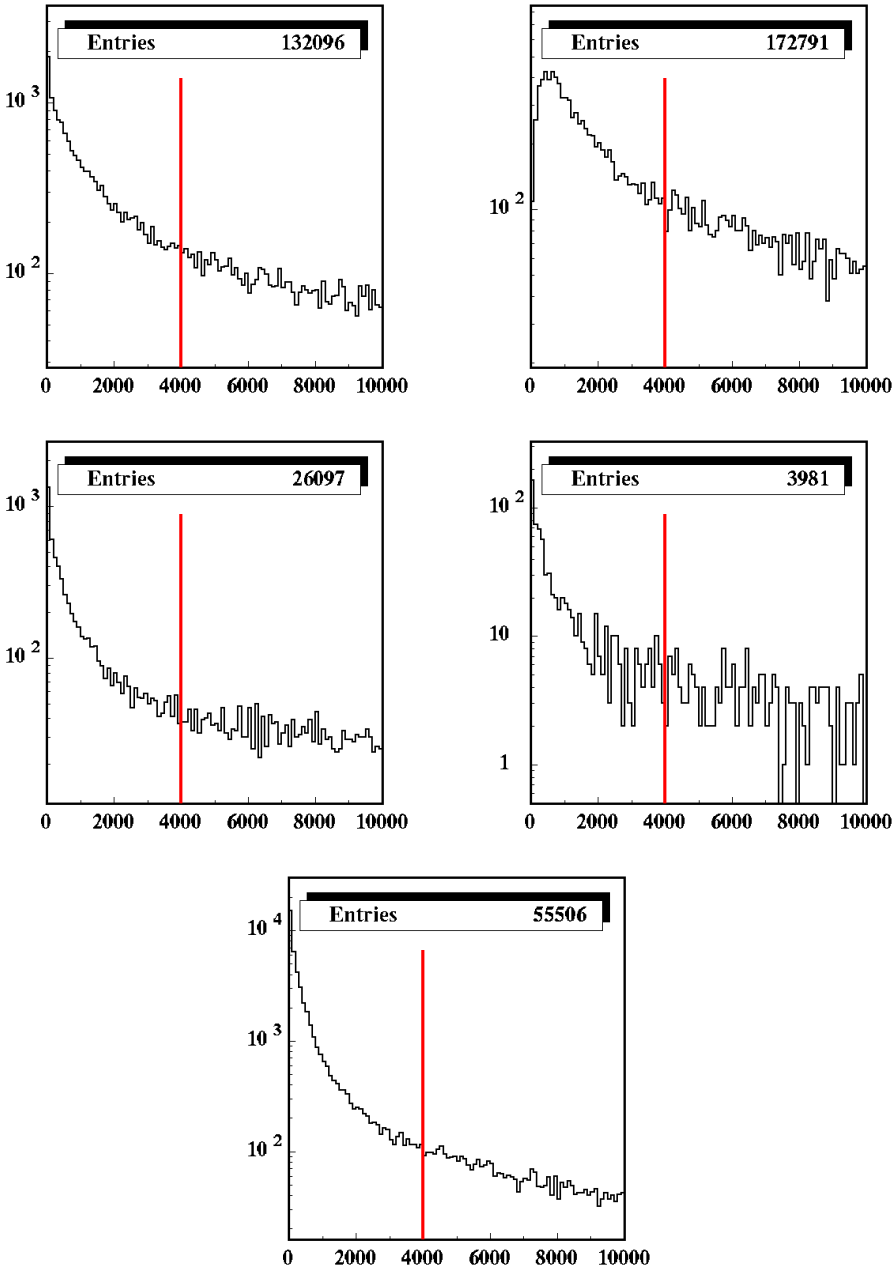

Fig. 3. Distribution of kinematic fit χ^2 after "low θ" cut. Top left: data; top right: `all_phys` Monte Carlo; center left: `allrad` Monte Carlo; center right: offpeak data; bottom: signal Monte Carlo. The red lines show the cut applied.

or:

$$M_{ee}(DC) < 30\ MeV \text{ and} \tag{12}$$
$$D_{ee}(DC) < 2\ cm\ . \tag{13}$$

The effect of these cuts are shown in figure 5 and 6. The band with low M_{ee} values and $D_{ee} < 10$ cm, visible in data, is due to a fraction of the $\phi \to K\bar{K}/\rho\pi$

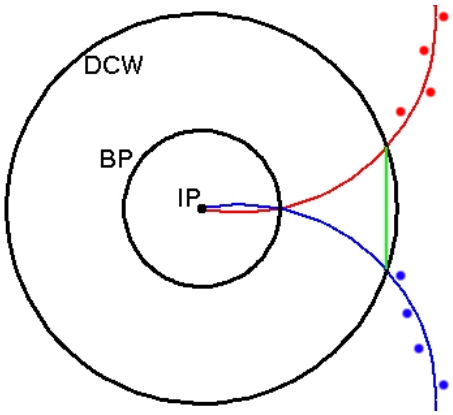

Fig. 4. Pictorial view of the x-y plane for an event with photon conversion on the beam pipe. ¡ The dots represent the hits in the DC. The tracks in the drift chamber can be backward extrapolated to the interaction point, mimicking the signal.

residual background contamination. These events are rejected by the time of flight cut described in the following sub-section.

5.5 Particle identification using the time of flight

Last, we use the Time of Flight (ToF) of the particles to identify their mass and apply a cut. The algorithm for particle identification is the same described in [2].
We require to have at least one particle identified as electron and we reject events having two or more particles identified as pion (see figure 7):

$$N_{electron} \geq 1 \quad \text{and} \tag{14}$$
$$N_{pion} \leq 1 \; . \tag{15}$$

6 BR evaluation

The result of all the background rejections cuts can be seen in figure 8, showing the four lepton invariant mass, $M_{e^+e^-e^+e^-}$, before and after analysis cuts. Background from kaons and $\rho\pi$ is almost disappeared; the same holds for background from η decays but for $\eta \to e^+e^-\gamma$, where $\sim 20\%$ of the events survive conversion cuts.

The counting of signal events is done subtracting background from ϕ decays and then fitting the two residual contributions: signal and continuum events.

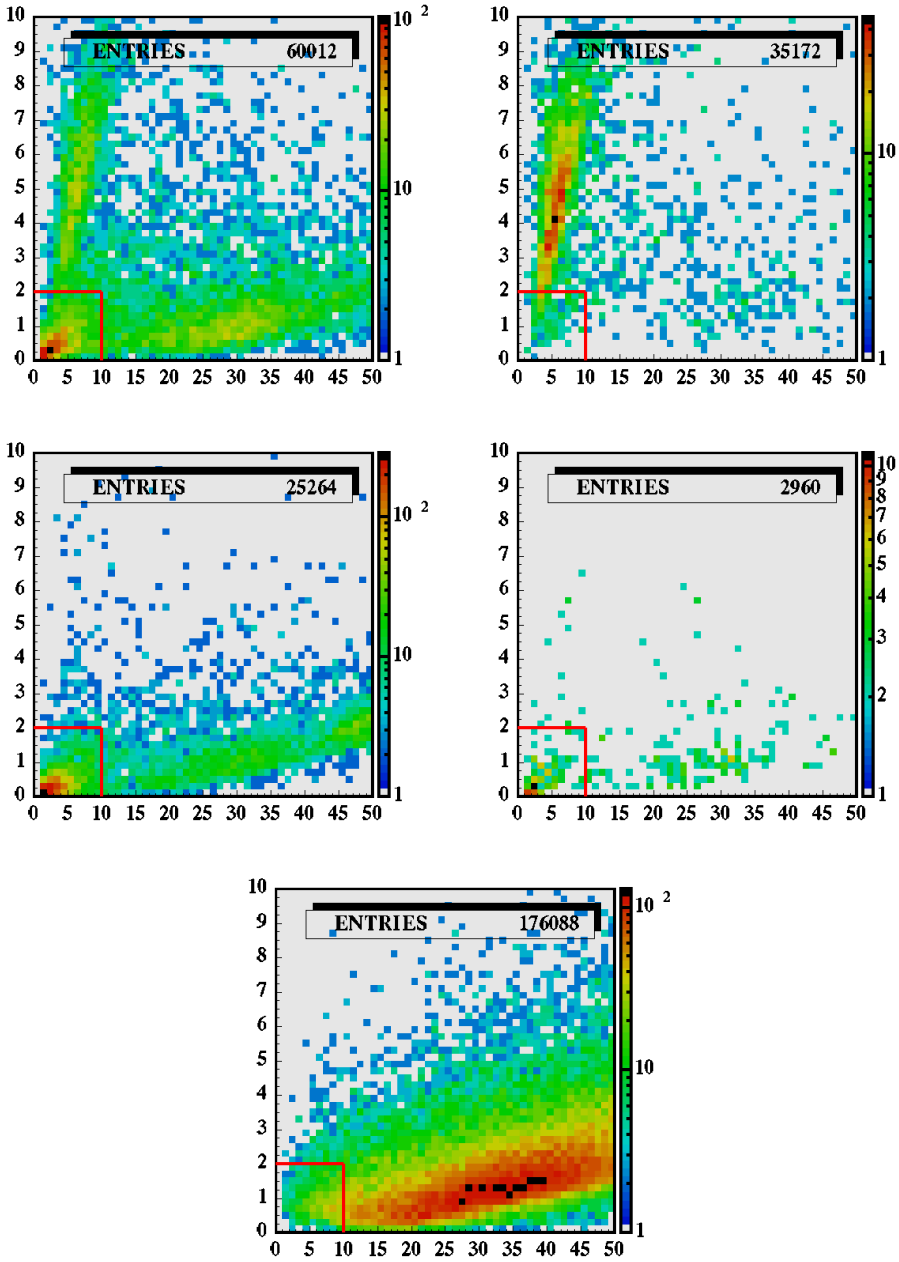

Fig. 5. Distance between lepton pairs (D_{ee}) versus reconstructed invariant mass (M_{ee}) for tracks extrapolated backward to the beam pipe. Pairs coming from photon conversion should ideally have $D_{ee} = 0$ and $M_{ee} = 0$. The plots contain only events surviving *s4p*, "low θ" and χ^2 cuts. Top left: data; top right: `all_phys` Monte Carlo; center left: `allrad` Monte Carlo; center right: offpeak data; bottom: signal Monte Carlo. The red lines show the cut applied.

The four lepton invariant mass, $M_{e^+e^-e^+e^-}$, for data and the expected backgrounds from ϕ decays are reported in figure 9, top left panel. The only significant source of contamination are about 80 $\eta \to e^+e^-\gamma$ events, that have the same shape of the signal. This is the reason for subtracting background

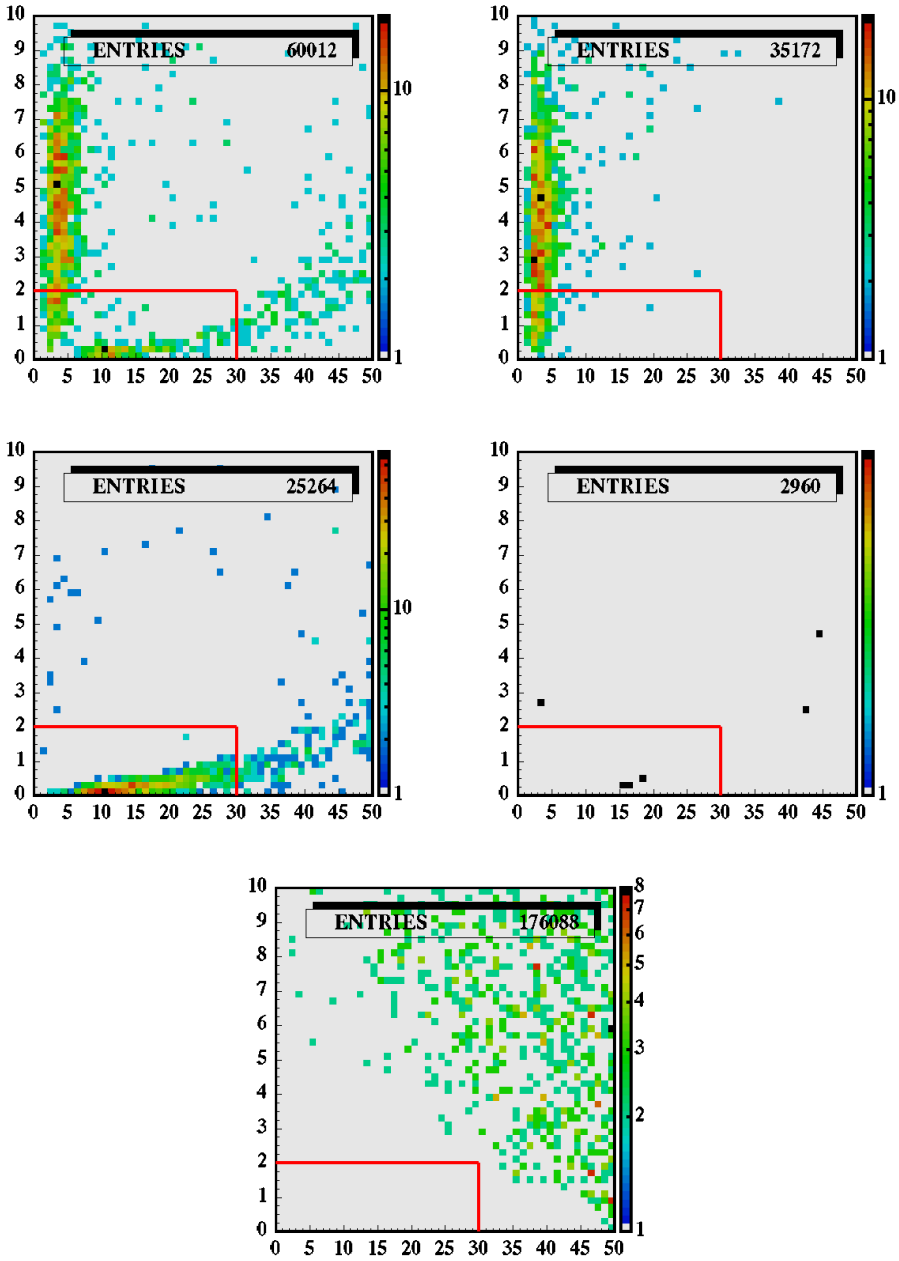

Fig. 6. Distance between lepton pair (D_{ee}) versus reconstructed invariant mass (M_{ee}) for tracks extrapolated backward to the drift chamber wall. Pairs coming from photon conversion should ideally have $D_{ee} = 0$ and $M_{ee} = 0$. The plots contain only events surviving $s4p$, "low θ" and χ^2 cuts. Top left: data; top right: `all_phys` Monte Carlo; center left: `allrad` Monte Carlo; center right: offpeak data; bottom: signal Monte Carlo. The red lines show the cut applied.

from ϕ decays before performing the fit. The $M_{e^+e^-e^+e^-}$ shape for signal is obtained by fitting MC events. The fit is done with a double gaussian in the region $532 < M_{e^+e^-e^+e^-} < 560$ MeV plus a third order polynomial function for lower values of the invariant mass. As shown in figure 9 top right panel,

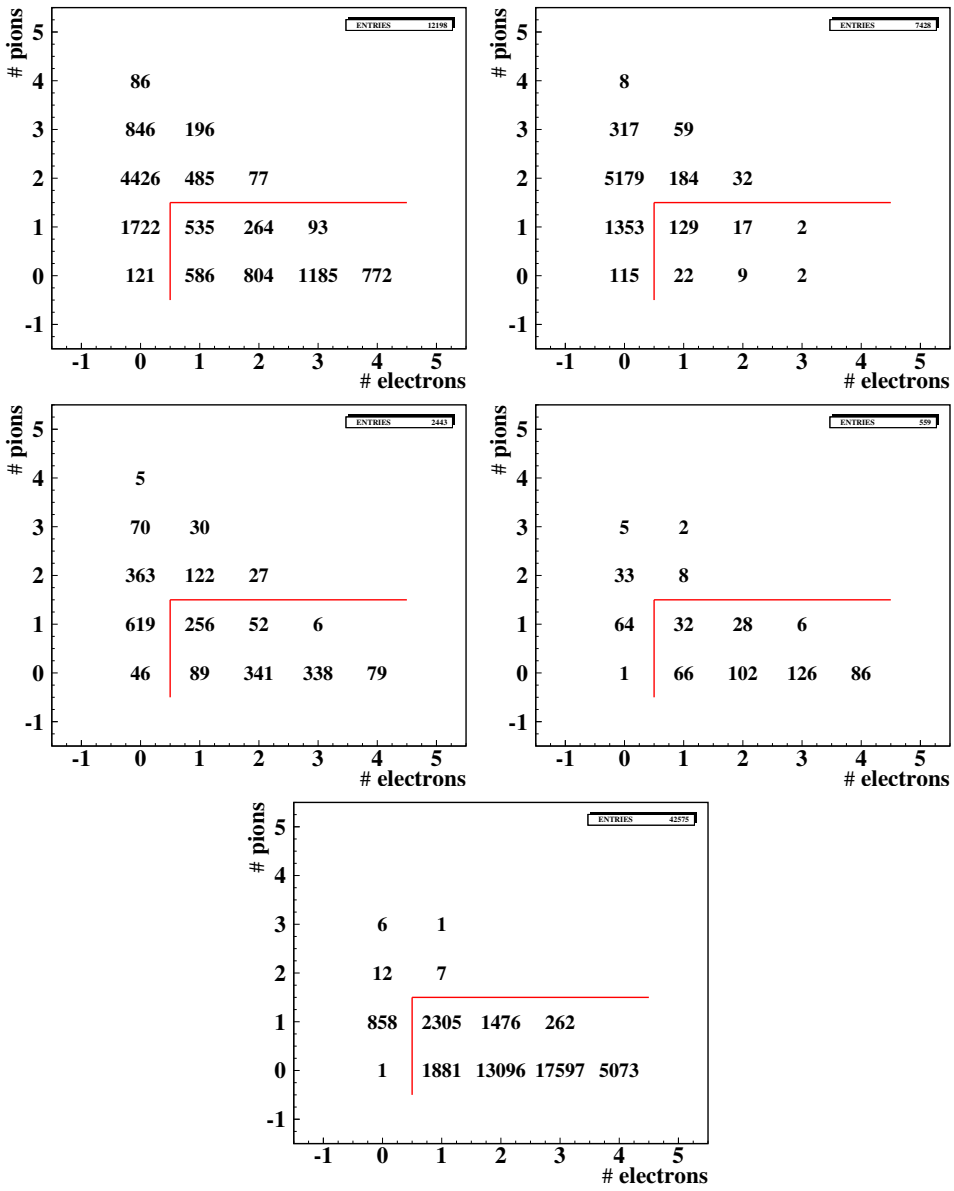

Fig. 7. Results of the time of flight particle identification. The plots contain only events surviving *s4p*, "low θ", χ^2 and conversion cuts. Top left: data; top right: `all_phys` Monte Carlo; center left: `allrad` Monte Carlo; center right: offpeak data; bottom: signal Monte Carlo. The red lines show the cut applied.

the MC shape is accurately reproduced. The $M_{e^+e^-e^+e^-}$ distribution for continuum events has been studied using data taken at $\sqrt{s} = 1$ GeV, where contributions from ϕ decays are suppressed. Unfortunately, the small statistics of the sample does not allow to precisely extract the shape. Anyhow, a first order polynomial function well reproduces data in the signal region (see bottom left panel of figure 9). The fit to the $M_{e^+e^-e^+e^-}$ distribution for data, after subtracting the resonant background, is done with the analytical function describing the $M_{e^+e^-e^+e^-}$ shape for signal events plus a first order polynomial. The free parameters are an overall scale factor for signal and the

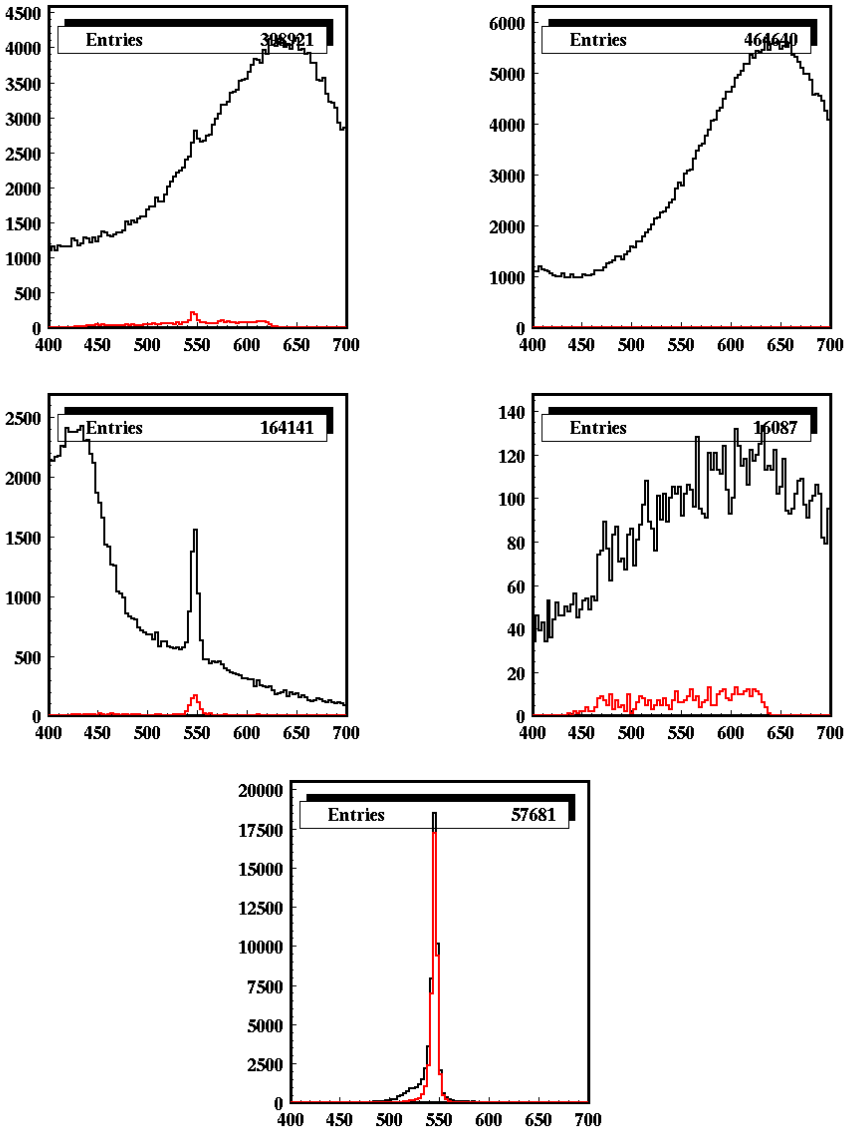

Fig. 8. Invariant mass of the four electrons before (black) and after (red) the background rejection cuts. Top left: data; top right: `all_phys` Monte Carlo; center left: `allrad` Monte Carlo; center right: offpeak data; bottom: signal Monte Carlo.

two parameters describing the continuum background. Fit results are shown in figure 9, bottom right panel. The resulting χ^2/ndf is 43.9/34, corresponding to Prob(χ^2) = 12%. The extracted number of events for signal is:

$$N(\eta \to e^+e^-e^+e^-) = 362 \pm 29\,. \tag{16}$$

The error on $N(\eta \to e^+e^-e^+e^-)$ is fully dominated by the statistics. The branching ratio (BR) of the $\eta \to e^+e^-e^+e^-(\gamma)$ decay is evaluated according

Source of uncertainty	Relative error
χ^2	$-0.51\% \,/\, +2.62\%$
$\cos\theta$	$-0.04\% \,/\, +0.47\%$
$s4p$	$+0.11\%$
$D_{ee}(BP)$	-0.64%
$M_{ee}(BP)$	$+2.42\%$
$D_{ee}(DC)$	——
$M_{ee}(DC)$	$-0.38\% \,/\, +0.24\%$
PID	$+1.84\%$
Fit range	$-0.38\% \,/\, +1.13\%$
Binning on $M_{e^+e^-e^+e^-}$	$-3.21\% \,/\, +0.19\%$
Background slope	$+0.38\%$
Total	$-3.35\% \,/\, +4.22\%$

Table 4
Summary of systematic uncertainties.

to the formula:

$$BR(\eta \to e^+e^-e^+e^-(\gamma)) = \frac{N_{\eta\to e^+e^-e^+e^-}}{N_{\eta\gamma}} \cdot \frac{1}{\epsilon_{\eta\to e^+e^-e^+e^-(\gamma)}}\,, \qquad (17)$$

where the analysis efficiency, $\epsilon_{\eta\to e^+e^-e^+e^-(\gamma)} = (20.46 \pm 0.09)\%$, has been evaluated using MC signal events. $N_{\eta\gamma}$ is the number of $\phi \to \eta\gamma$ events produced in the analyzed data sample: $N_{\eta\gamma} = \mathcal{L} \cdot \sigma_{\phi\to\eta\gamma}$. The luminosity, $\mathcal{L} = (1733 \pm 10)$ pb^{-1}, is evaluated using large angle Bhabha scattering events [19], while the cross section, $\sigma_{\phi\to\eta\gamma} = (41.7 \pm 0.6)$ nb, accounts for the ϕ meson line shape [20]. The resulting BR is:

$$BR(\eta \to e^+e^-e^+e^-(\gamma)) = (2.44 \pm 0.19_{\text{stat.}} \pm 0.04_{\text{norm.}}) \cdot 10^{-5}\,. \qquad (18)$$

The second error includes uncertainties on $\epsilon_{\eta\to e^+e^-e^+e^-(\gamma)}$, $\mathcal{L}$, and $\sigma_{\phi\to\eta\gamma}$.

7 Evaluation of the systematic uncertainties

The systematic uncertainties of analysis cuts have been evaluated by applying separately a variation of $\pm 1\,\sigma$ on all variables and re-evaluating the branching ratio. The σ value has been obtained using MC signal events. For the χ^2 variable the cut has been moved by ± 500, while for particle identification the

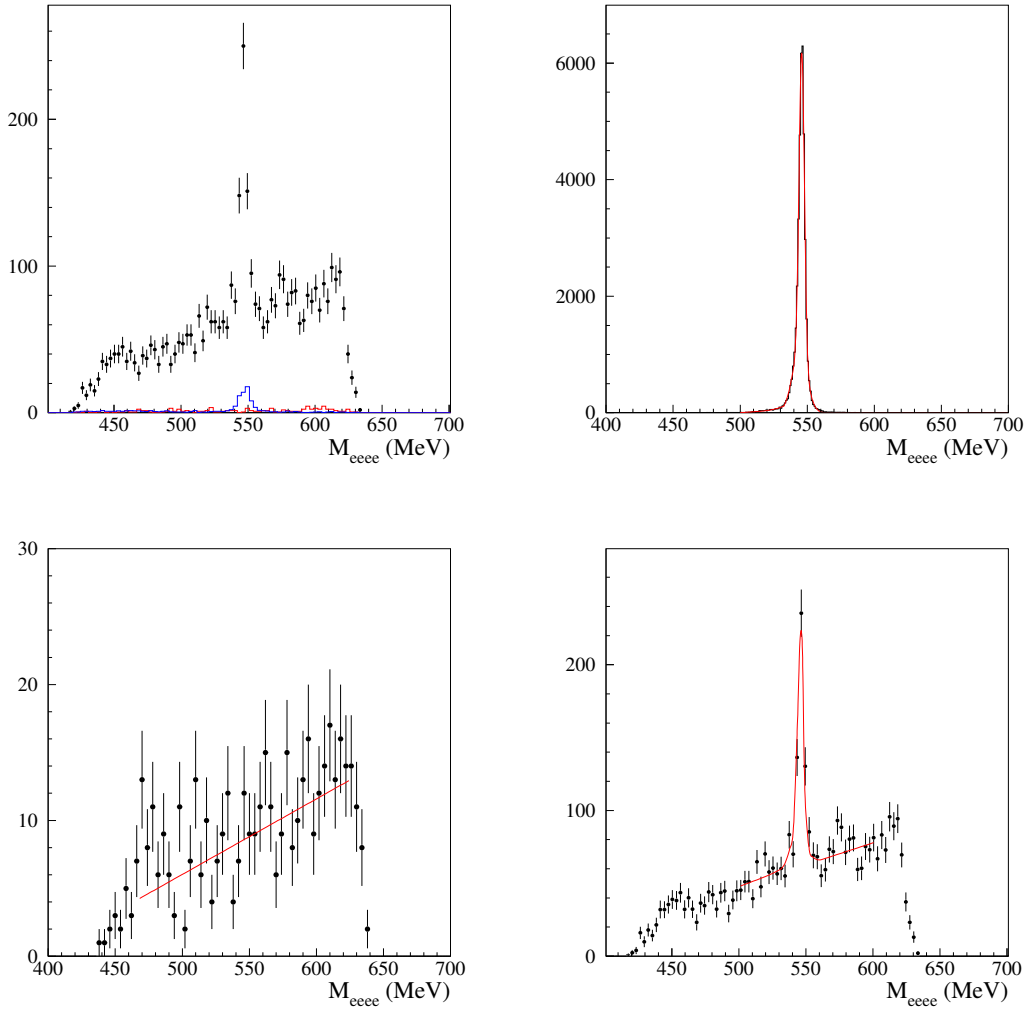

Fig. 9. Top left: distribution of $M_{e^+e^-e^+e^-}$ after all analysis cuts for data. Residual background contributions from $\phi \to \eta\gamma$ and $\phi \to K\bar{K}/\pi^+\pi^-\pi^0$ are displayed in blue and red respectively. Top right: fit to the $M_{e^+e^-e^+e^-}$ shape for MC signal events; bottom left: fit to the $M_{e^+e^-e^+e^-}$ distribution for offpeak data with a first order polynomial; bottom right: fit to the $M_{e^+e^-e^+e^-}$ spectrum with the expected contributions from signal and continuum events.

slope used to separate pions from electron has been changed by $\pm 10\%$. In case of variations of the same sign, the maximum difference has been taken as uncertainty. Systematic errors on the fit to the $M_{e^+e^-e^+e^-}$ distribution are evaluated in the following way:

- the binning of the $M_{e^+e^-e^+e^-}$ histogram has been modified from 3 MeV, used as default, to 2 and 4 MeV;
- the standard fit range, $500 < M_{e^+e^-e^+e^-} < 600$ MeV has been enlarged and reduced by 10 MeV on both sides;
- the slope of the continuum background has been fixed to the value obtained

Source of uncertainty	Relative error
χ^2	$-0.51\% \ / + 2.62\%$
$\cos\theta$	$-0.04\% \ / + 0.47\%$
$s4p$	$+0.11\%$
$D_{ee}(BP)$	-0.64%
$M_{ee}(BP)$	$+2.42\%$
$D_{ee}(DC)$	——
$M_{ee}(DC)$	$-0.38\% \ / + 0.24\%$
PID	$+1.84\%$
Fit range	$-0.38\% \ / + 1.13\%$
Binning on $M_{e^+e^-e^+e^-}$	$-3.21\% \ / + 0.19\%$
Background slope	$+0.38\%$
Total	$-3.35\% \ / + 4.22\%$

Table 5
Summary of systematic uncertainties.

from offpeak data.

Relative errors for all systematics are reported in table 5. The total error has been obtained as the quadratic sum of all contributions. Taking it into account, the measurement of the branching ratio for the $\eta \to e^+e^-e^+e^-(\gamma)$ channel results:

$$BR(\eta \to e^+e^-e^+e^-(\gamma)) = (2.44 \pm 0.19_{\text{stat.}} \pm 0.04_{\text{norm.}} \, ^{+0.10}_{-0.08 \text{ syst.}}) \times 10^{-5} \, . \quad (19)$$

8 Checks on background

The $\eta \to e^+e^-\gamma$ background with photon conversion is the only relevant residual background contamination at the end of the analysis chain. This channel has the same $M_{e^+e^-e^+e^-}$ distribution of the signal, therefore it is important to have it under control. Studying background from photon conversion for $\phi \to \eta e^+e^-$ events, a relevant contribution coming from the region $D_{ee}(DC) \sim 2.5$ cm, $M_{ee}(DC) \sim 60$ MeV is observed [21]. It is also present in our Monte Carlo simulations and can be completely removed by rejecting events with $D_{ee}(DC) < 10$ cm and $M_{ee}(DC) < 80$ MeV. For the $\eta \to e^+e^-e^+e^-(\gamma)$ channel this cut cannot be applied because, having two

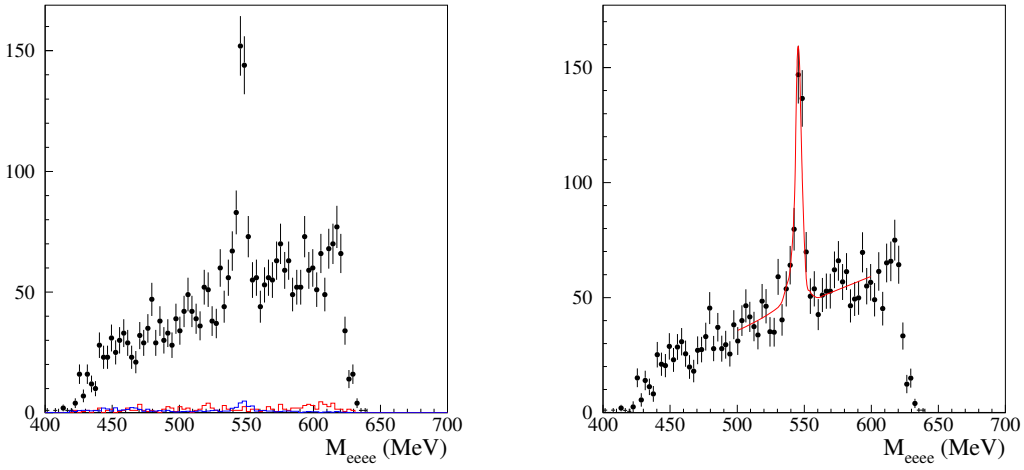

Fig. 10. Left: distribution of $M_{e^+e^-e^+e^-}$ for data with hardened cuts on photon conversions. Residual background contributions from $\phi \to \eta\gamma$ and $\phi \to K\bar{K}/\pi^+\pi^-\pi^0$ are displayed in blue and red respectively. Right: fit to $M_{e^+e^-e^+e^-}$ distribution after background subtraction.

electrons and two positrons in the final state, the search for conversions is done for all the four e^+e^- combinations, thus spreading the signal contribution in the $M_{ee}(DC)$-$D_{ee}(DC)$ plane. Anyhow, just as a cross-check, we have added this cut to our analysis, and re-evaluated the branching ratio. As shown in figure 10 left panel, this cut strongly reduces background contamination from $\eta \to e^+e^-\gamma$. The number of signal events extracted by the fit (figure 10 right panel) decreases by 25%, $N(\eta \to e^+e^-e^+e^-(\gamma)) = 271 \pm 25$, and the branching ratio becomes $BR(\eta \to e^+e^-e^+e^-(\gamma)) = (2.52 \pm 0.23_{\text{stat.}}) \times 10^{-5}$, well in agreement with our measurement.

In order to check for bias introduced when cutting on time of flight variables, the branching ratio has also been evaluated removing the ToF requirements. As shown in figure 11 left, the background from $\phi \to K\bar{K}/\pi^+\pi^-\pi^0$ increases noticeably, and also larger contributions from $\phi \to \eta\gamma$ decays are present. The number of signal events extracted from the fit to $M_{e^+e^-e^+e^-}$ (figure 11 right) is $N(\eta \to e^+e^-e^+e^-(\gamma)) = 421 \pm 50$, and the branching ratio becomes $BR(\eta \to e^+e^-e^+e^-(\gamma)) = (2.57 \pm 0.31_{\text{stat.}}) \times 10^{-5}$, again well in agreement with our measurement.

Acknowledgments

We would like to thank all those who helped during this work with discussions, suggestions, support and in any other possible way. In particular we would like to mention Johan Bijnens for the useful discussions and for having provided his

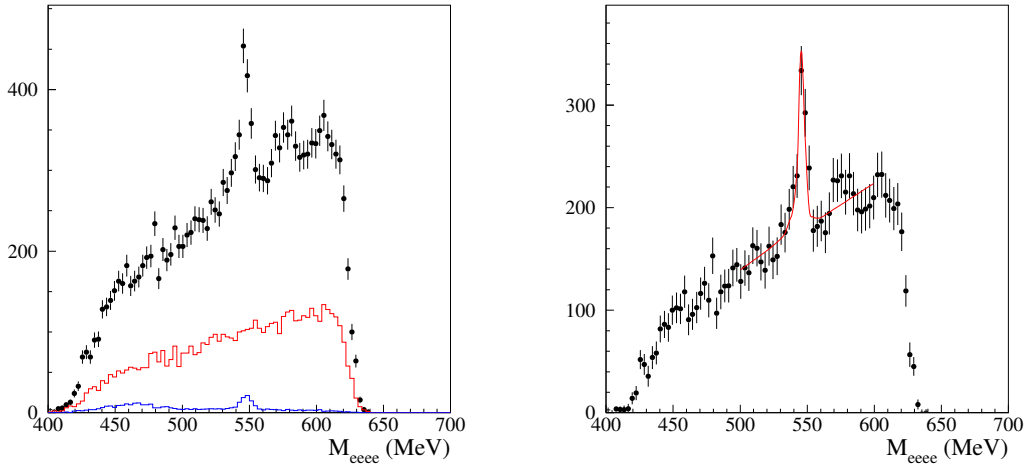

Fig. 11. Left: distribution of $M_{e^+e^-e^+e^-}$ for data when removing the cut on time of flight. Residual background contributions from $\phi \to \eta\gamma$ and $\phi \to K\bar{K}/\pi^+\pi^-\pi^0$ are displayed in blue and red respectively. Right: fit to $M_{e^+e^-e^+e^-}$ distribution after background subtraction.

own code, Claudio Gatti for the development of the Monte Carlo generator, Biagio Di Micco for the help during its test and Antonio De Santis for the work done together on the tracking efficiency. We would like also to thank our referees, Caterina Bloise and Antonio Passeri, for useful discussions and for a careful review of this work.

References

[1] F. Ambrosino *et al.* [KLOE Collaboration], Phys. Lett. B **675** (2009) 283

[2] S. Giovannella and R. Versaci, KLOE memo 350 (2008)

[3] L. G. Landsberg, Phys. Rept. **128** (1985) 301.

[4] T. Miyazaki and E. Takasugi, Phys. Rev. D **8**, 2051 (1973).

[5] J. Bijnens and F. Perrsson, arXiv:hep-ph/0106130.

[6] C. C. Lih, arXiv:0912.2147 [hep-ph].

[7] T. Petri, PhD thesis, arXiv:1010.2378 [nucl-th].

[8] Jarlskog, C., & Pilkuhn, H., Nucl. Phys. B **1** (1967) 264.

[9] R. R. Akhmetshin *et al.* [CMD-2 Collaboration], Phys. Lett. B **501** (2001) 191 [arXiv:hep-ex/0012039].

[10] M. Berlowski *et al.*, Phys. Rev. D **77** (2008) 032004.

[11] K. Nakamura et al. [Particle Data Group], J. Phys. G **37**, 075021 (2010)

[12] S. Giovannella and R. Versaci, KLOE memo 329 (2008)

[13] R. Versaci, KLOE memo 358 (2009)

[14] A. De Santis and R. Versaci, KLOE memo 356 (2009)

[15] E. Barberio and Z. Was, Comput. Phys. Commun. **79** (1994) 291.

[16] M. Martini and S. Miscetti, KLOE memo 342 (2007)

[17] A. De Santis and R. Versaci, KLOE memo 343 (2008)

[18] C. Gatti, PhD thesis (2003)

[19] F. Ambrosino et al. [KLOE Collaboration], Eur. Phys. J. C 47 589 (2006)

[20] S. Giovannella and S. Miscetti, KLOE note 212 (2006)

[21] S. Giovannella on behalf of the KLOE-2 Collaboration, proceedings of DISCRETE 2010 - Symposium on Prospects in the Physics of Discrete Symmetries, to be published in *Journal of Physics: Conference Series*